

**DETECTION OF A SUPER STAR CLUSTER AS THE  
IONIZING SOURCE IN THE LOW LUMINOSITY AGN  
NGC 4303**

Luis Colina<sup>1</sup>, Rosa Gonzalez Delgado<sup>2</sup>, J. Miguel Mas-Hesse<sup>3</sup>, Claus Leitherer<sup>4</sup>

(1) *Instituto de Estructura de la Materia (CSIC), Serrano 121, 28006 Madrid, Spain (colina@isis.iem.csic.es)*

(2) *Instituto de Astrofísica de Andalucía (CSIC), P.O. Box 3004, 18080 Granada, Spain (rosa@iaa.es)*

(3) *Laboratorio de Astrofísica Espacial y Física Fundamental, INTA, P.O. Box 50727, 28080 Madrid, Spain  
(mm@laeff.esa.es)*

(4) *Space Telescope Institute, 3700 San Martin Drive, Baltimore, MD 21218, USA (leitherer@stsci.edu)*

1

Received \_\_\_\_\_; accepted \_\_\_\_\_

---

<sup>1</sup>Based on observations with the NASA/ESA *Hubble Space Telescope*, obtained at the Space Telescope Science Institute, which is operated by the Association of universities for Research in Astronomy, Inc., under NASA contract NAS 5-26555. Based on observations with the William Herschel Telescope operated on the island of La Palma by the ING in the Spanish Observatorio del Roque de los Muchachos of the Instituto de Astrofísica de Canarias.

## ABSTRACT

Hubble Space Telescope (HST) ultraviolet STIS imaging and spectroscopy of the low luminosity AGN (LLAGN) NGC 4303 have identified the previously detected UV-bright nucleus of this galaxy, as a compact, massive and luminous stellar cluster. The cluster with a size (FWHM) of 3.1 pc, and an ultraviolet luminosity  $\log L_{1500\text{\AA}} (\text{erg s}^{-1} \text{\AA}^{-1}) = 38.33$  is identified as a nuclear super star cluster (SSC) like those detected in the circumnuclear regions of spirals and starburst galaxies. The UV spectrum showing the characteristic broad P Cygni lines produced by the winds of massive young stars, is best fitted by the spectral energy distribution of a massive cluster of  $10^5 M_{\odot}$  (for a Salpeter IMF law with lower-mass cutoff of  $1 M_{\odot}$ ) generated in an instantaneous burst 4 Myr ago. The ionizing energy produced by this cluster exceeds the flux needed to explain the nuclear H $\alpha$  luminosity. No evidence for an additional non-thermal ionizing source associated with an accreting black hole is detected in the ultraviolet. These new HST/STIS results show unambiguously the presence of a compact, super star cluster in the nucleus of a low luminosity AGN, that is also its dominant ionizing source. We hypothesize that at least some LLAGNs in spirals could be understood as the result of the combined ionizing radiation emitted by an evolving SSC (i.e. determined by the mass and age) and a black hole (BH) accreting with low radiative efficiency (i.e. radiating at low sub-Eddington luminosities), coexisting in the inner few parsecs region. Complementary multifrequency studies give the first hints of the very complex structure of the central 10 pc of NGC 4303 where a young SSC apparently coexists with a low efficiency accreting black hole and with an intermediate/old compact star cluster, and where in addition an evolved starburst could also be present. If structures as such detected in NGC 4303 are common in the nuclei of

spirals, the modeling of the different stellar components, and their contribution to the dynamical mass, has to be established accurately before deriving any firm conclusion about the mass of central black holes of few to several million solar masses.

*Subject headings:* — galaxies: active — galaxies: nuclei — galaxies: starburst — galaxies: individual (NGC 4303) — ultraviolet: galaxies

## 1. INTRODUCTION

Low luminosity Active Galactic Nuclei (LLAGNs) including low-luminosity Seyferts, classical LINERs, weak-[O I] LINERs, and LINER/HII transition-like objects are the most common type of galaxies showing nuclear activity. LINERs alone make up 50%–70% of AGNs and 20%–30% of all galaxies in surveys of nearby bright galaxies (Ho, Filippenko & Sargent 1997). It is therefore of fundamental importance to identify unambiguously the nature of the energy source in LLAGNs, and to quantify the contribution of stars and accreting black-holes to their energy output.

Recent X-ray observations of LLAGNs confirm that some LINERs are the low luminosity end of the luminous AGN phenomenon identified in Seyfert 1 and QSOs where accreting black-holes are the dominant energy source (Ho et al. 2001; Eracleous et al. 2002), while in others the energy output seems to be dominated by powerful starbursts (Terashima et al. 2000; Eracleous et al. 2002). HST ultraviolet imaging and spectroscopy has shown the presence of young massive stars at various scales in AGNs. Seyfert 2 galaxies known to have bright kpc-size star-forming rings show that the AGN core is barely detected in the UV, and that the massive stars dominate the observed circumnuclear UV emission (Colina et al. 1997a). The detection of stellar winds and photospheric absorption lines in the ultraviolet spectra of Seyfert 2 galaxies (Heckman et al. 1997; González Delgado et al. 1998) has proven unequivocally the presence of clusters of massive young stars in the circumnuclear regions of these galaxies. These nuclear starbursts are dusty star-forming regions of a few hundred parsecs in size and with an average age of 3 to 6 Myrs (González Delgado et al. 1998). Optical and UV studies of Seyfert 2 galaxies have detected the presence of young massive starbursts within 300 pc of the nucleus in 30% to 50% of the galaxies investigated (Cid Fernandes et al. 2001 and references therein). Finally, the compact ultraviolet sources detected in some UV bright LINERs are nuclear star clusters with sizes of about 10-15 pc

like in NGC 4569 (Maoz et al. 1998; Barth et al. 1998).

In summary, recent evidence collected mainly with HST and *Chandra* indicates the presence of massive stellar clusters in the circumnuclear regions (few to several hundred parsecs) in a large fraction of LINERs and Seyfert 2 galaxies, that substantially contribute to their energy output. However, the fundamental question of whether or not massive stellar clusters exist in the central few pc region, i.e. nucleus, of LLAGNs contributing substantially, or even dominating, the energy output, requires detailed investigations in selected nearby galaxies like NGC 4303.

NGC 4303 (M 61) is a barred spiral classified as SAB(rs)bc (de Vaucouleurs et al. 1991) and located in the Virgo cluster (adopted distance of 16.1 Mpc hereinafter; see also Colina et al. 1997b). Multi-wavelength HST images of NGC 4303 have unveiled the presence of a nuclear stellar bar of 250 pc in size centered on a bright optical and near-IR nucleus<sup>2</sup>, itself connected with a nuclear star-forming spiral of about 250 pc in radius. (Colina et al. 1997b; Colina & Arribas 1999; Colina & Wada 2000). The UV luminosity of the spiral dominates the observed integrated UV output. The brightest knots delineating the spiral have observed UV luminosities  $L(2200\text{\AA}) \sim 2 \times 10^{37} \text{ erg s}^{-1} \text{ \AA}^{-1}$  similar to that of the R136 cluster in 30 Doradus (Vacca et al. 1995), and in the high UV luminosity end of the distribution function of compact stellar clusters detected in star-forming rings (Maoz et al. 1996).

The 2D velocity field of the warm ionized gas and cold molecular gas shows that the nucleus is also the dynamical center of a disk of 300 pc in radius, and in which the star-forming spiral is embedded (Colina & Arribas 1999; Schinnerer et al. 2002; Colina et

---

<sup>2</sup>throughout the paper we distinguish between nucleus, nuclear and circumnuclear regions each indicating different physical sizes of about 0.01, 0.1 and 1 kpc, respectively

al. 2002, unpublished). Ground-based spectroscopy reveals that the optical emission lines emitted by the nuclear region ( $\sim 100$  pc size) have ratios in the borderline of Seyfert 2 and LINER nuclei (Colina & Arribas 1999). These observations confirm that the bright nucleus of NGC 4303 is a low luminosity AGN and is indeed located at the true center of the galaxy.

## 2. OBSERVATIONS

Ultraviolet imaging and spectroscopy of NGC 4303 was obtained using STIS onboard HST. The ultraviolet image was taken on July 7th, 2000 through filter F25Q1Z ( $\lambda_p = 2364.8\text{\AA}$ ) for a total integration time of 2080 seconds. Spectroscopy was done on February 12th, 2001 with the  $52''0 \times 0''2$  long-slit and G140L grating covering the 1100-1700 $\text{\AA}$  spectral range with a dispersion of  $0.6\text{\AA}/\text{pix}$ . The roll angle of the telescope during the observations was such that the slit was oriented along position angle 220 degrees, i.e. along the line connecting the UV-bright nucleus of NGC 4303 with the brightest circumnuclear stellar cluster as identified in the previous HST/WFPC2 ultraviolet image (cluster G; Colina et al. 1997b). Total integration time for the spectroscopy was 13442 seconds divided in five individual exposures taken during five contiguous orbits, and using therefore the same guide stars. The individual imaging and spectroscopic exposures were dithered and therefore they were calibrated independently with the standard STIS calibration pipeline using the most updated calibration files. The individual images and spectra were combined afterwards to generate the final image and long-slit spectrum.

A high signal-to-noise long-slit optical spectrum was obtained with the ISIS double spectrograph attached at the William Herschel Telescope during an observatory service observing run on May 29th, 2001. The  $1''0$  wide slit was oriented along position angle 220 degrees on the sky to cover the nucleus and circumnuclear clusters. The total integration time was 3600 seconds, split in three equal exposures of 1200 seconds, each. The seeing

conditions were stable and values of  $1''.5 - 2''.0$  were measured. The final spectra were obtained combining two independent blue (3600–6280 Å) and red (6205–6990) spectral ranges taken simultaneously with the two-arm spectrograph. The spectral dispersion was  $0.8\text{Å}/\text{pix}$  and  $0.9\text{Å}/\text{pix}$  for the red and blue ranges of the spectrum, respectively. Calibration was done following standard long-slit spectroscopic procedures. These data are used here only to measure the  $\text{H}\alpha$  nuclear flux, and to obtain a new determination of the optical emission line ratios (see Table 1). Although the airmass was in the 1.3 to 1.55 range during the observations, atmospheric differential refraction has no effect on the emission line ratios since the slit was positioned close to the parallactic angle (off by up to 10 degrees).

### 3. RESULTS

The high-resolution ( $0''.025$  per pixel) deep STIS ultraviolet image (Figure 1) shows in much more detail the structure already detected in a previous lower resolution ( $0''.1$  per pixel) WFPC2 image (Colina et al. 1997b). Each of the previously unresolved star-forming knots located in the circumnuclear spiral structure, breaks now into several smaller, fainter knots separated by distances of less than  $0''.2$  (i.e.  $\leq 15$  pc; see Figure 1, and WFPC2 UV image in Colina 1997b for a comparison). However, the UV-bright nucleus, unresolved in our previous WFPC2 image, remains as a compact source. Although a full analysis of the STIS image is beyond the scope of this paper and the results will be published elsewhere (Colina et al. in preparation), it is relevant for the purpose of this paper to establish the size of the compact UV-bright nucleus. The STIS PSF for the filter F25Q7Z was modeled using Tiny Tim version 6.0 (Krist & Hook 2001) and assuming a flat spectrum ( $F_\lambda = \text{constant}$ ) source. Encircled energy measurements and two-dimensional gaussian fits to the core of the Tiny Tim PSF light profile were performed, and subsequently compared with the results obtained for the observed light distribution of the UV-bright nucleus. The results of this

analysis allows one to conclude that the nucleus of NGC 4303 is resolved and has a size (FWHM) of  $0''.040 (\pm 0''.005)$  in the UV, equivalent to 3.1 pc at the assumed distance of NGC 4303. In addition, simulations of extended sources of various sizes convolved with the modeled Tiny Tim PSF were also performed. For these simulations, the modeled PSF was computed considering a subsampling factor of 5, i.e.  $0''.005$  per pixel. Extended sources were simulated as regions of constant surface brightness with diameters ranging from  $0''.015$  to  $0''.055$ . The extended sources were convolved with the subsampled PSF and the resulting images were rebinned by a factor 5 to generate the final simulated images with a pixel size of  $0''.025$ , i.e. the pixel scale of STIS detectors in the ultraviolet. As before, encircled energy measurements and two-dimensional gaussian fits were performed on the rebinned images. The size of the nucleus obtained in this way is consistent with the value derived from the previous analysis, and corresponds to that of an extended region of  $0''.045$  in diameter.

The STIS UV long-slit spectrum along PA 220 shows three independent spectra associated with the nucleus, the brightest circumnuclear cluster (cluster G after Colina 1997b), and a fainter cluster (cluster L, not previously identified). The one-dimensional spectra from the nucleus, cluster G and cluster L were extracted from the long-slit spectrum using apertures of  $0''.9$ ,  $0''.8$  and  $0''.5$ , respectively. The three spectra are almost indistinguishable (see Figure 2) showing all of them very prominently the characteristic broad P Cygni lines (N V  $1240\text{\AA}$ , Si IV  $1400\text{\AA}$ , C IV  $1550\text{\AA}$ ) produced by the winds of massive young stars. In addition, the three spectra show a narrow Ly $\alpha$  line in emission but no trace of other strong emission lines like Si IV  $1400\text{\AA}$ , C IV  $1550\text{\AA}$ , and He II  $1640\text{\AA}$  typical of luminous Seyfert 2 galaxies like NGC 1068 (Crenshaw & Kraemer 2000), or gas heated by fast shocks (Allen et al. 1998).

In order to establish the age and mass of the stellar clusters, as well as the internal absorption towards them, a detailed comparison of the observed and synthetic ultraviolet

spectra has been performed assuming a given extinction law. Differences between Calzetti’s law, derived from ultraviolet observations of starburst galaxies (Calzetti et al. 2000), and LMC extinction law can not be appreciate due to the small wavelength range covered by the STIS spectra. However, extinction in star-forming regions seems to follow an LMC or SMC-like law, i.e. with a rather weak bump at 2200 Å, independently of the metallicity of the region (Mas-Hesse & Kunth 1999). These authors concluded that the high ionizing flux produced by the young massive stars would destroy the graphite grains, which are responsible for the shape of the Galactic extinction law, leaving mostly silicates, whose extinction properties are closer to the shape of the LMC-SMC laws. Therefore, a LMC extinction law is used throughout the following analysis. The extinction values using Calzetti’s law are also given in Table 1 for completeness. The ages of the clusters have been obtained by comparing the observed profile of the P Cygni lines with the model predictions for solar metallicity stars. Synthetic spectra with metallicities lower than solar (obtained using a mix of LMC and SMC stellar libraries) do not reproduce the intense P Cygni lines detected in NGC 4303. Moreover, instantaneous bursts are preferred over continuous star formation because the Si IV 1400Å profile is better fitted by instantaneous bursts of a given age. Finally, once the age of the clusters and stellar upper mass of the initial mass function (IMF) are fixed, the mass and internal extinction of the clusters are derived by comparing the slopes of the observed and synthetic (stellar plus extinction) continua over the entire ultraviolet spectral range available to us.

Following the methodology outlined above, the UV spectrum of the nucleus with its prominent broad P Cygni lines is best fitted with the synthetic spectrum of an unobscured ( $E(B-V)= 0.07$  for an LMC extinction law), massive  $1 \times 10^5 M_{\odot}$ , 4 Myr old instantaneous starburst, with a Salpeter IMF in the 1 to  $100 M_{\odot}$  stellar mass range (see Figure 3 and Table 2). The circumnuclear clusters are similarly best fitted by unobscured, less massive ( $\sim 10^4 M_{\odot}$ ), younger (3 to 3.5 Myrs) clusters (see Table 2 for detailed parameters). The

best fit for cluster G requires an IMF characterized by a slope of 1.5, i.e. flatter than Salpeter, indicating the need for a large fraction of very massive stars to explain the UV spectral features. The need for a flat IMF does not necessarily imply an IMF different than Salpeter but could be understood if cluster G were extended and therefore, due to mass segregation within the cluster, we could be biased towards the more massive stars since the width of the slit is only of  $0''.2$  (i.e. 15.6 pc) and its orientation was selected along the line connecting the UV-bright nucleus and the UV-peak emission of cluster G.

Although the UV spectra of the nucleus and circumnuclear stellar clusters are almost indistinguishable, the optical emission line ratios derived from the WHT narrow long-slit spectrum show that the excitation conditions in the nucleus are clearly different from those present in the circumnuclear stellar clusters (see Figure 4 and Table 1). While the circumnuclear clusters show the typical emission line ratios of compact HII regions, the spectrum of the nucleus ( $1''.0 \times 1''.0$ ) is classified as a LINER or, due to the weakness of the [O I] 6300Å line, as a weak-[O I] LINER (Figure 4). However, our previous two-dimensional integral-field spectra identified the nucleus as a low-luminosity Seyfert 2/LINER borderline AGN (Colina & Arribas 1999). Discrepancies between these two classifications illustrate the difficulties in classifying LLAGNs, mostly due to the intrinsic uncertainties in ground-based measurements in general, i.e. positioning of a narrow slit ( $1''.0$ ), corrections in the Balmer emission lines due to stellar absorptions, structure and size of extended ionized gas, measurement of weak emission lines against the bright continuum emitted by the bulge population, etc. For NGC 4303, the structure of the ionized gas and the contribution of the  $H\beta$  line in absorption could be relevant factors working on opposite directions when computing the O III/ $H\beta$  ratio. The surface brightness of the  $H\beta$  and [O III] 5007Å lines along PA 220 indicates that the high-excitation [O III] emitting gas is more centrally concentrated than the low-excitation  $H\beta$  emitting gas, as traced by the steep gradient in the [O III] light distribution with the available  $0''.3$  pixel resolution. This could have an

important effect decreasing the [O III]/H $\beta$  ratio when obtaining the integrated spectrum for a region of 1".0 to 1".5 across. Therefore, this suggest that the [O III]/H $\beta$  ratio would increase if an spectrum sampling the central 0".1 were available. On the other hand, the nuclear optical continuum of NGC 4303 redwards of 4800Å can be fitted reasonably well with a 1 Gyr stellar population. The core of the corresponding stellar H $\beta$  absorption line with an equivalent width of 1.8Å will decrease the flux of the H $\beta$  nebular line by a factor of about two. If this correction were applied to the observed [O III]/H $\beta$  ratio, its value would drop by a factor 2 with respect to the value given in table 1. Therefore although the most recent ground-based spectra favors the classification of the LLAGN nucleus of NGC 4303 as a [O I]-weak LINER, the final classification will not be obtained until the new scheduled HST/STIS spectroscopic data, isolating the emission from the nucleus with a slit width of 0".2 and covering the entire 1200Å – 9000Å range, are taken.

Finally, the internal extinction towards the nucleus and circumnuclear stellar clusters is very low with E(B–V) values of less or equal than 0.1 as derived from the UV-shape of the spectrum (see Table 1 for specific values). These values agree with those derived from the H $\alpha$ /H $\beta$  line ratios after the fluxes of the nebular Balmer lines are corrected by an stellar absorption of 1.8Å(see above).

## 4. DISCUSSION

### 4.1. NGC 4303 nucleus: A LLAGN powered by super star cluster

The nuclear cluster characterized by its size of 3.1 pc, its mass of  $10^5 M_{\odot}$ , and its ultraviolet luminosity  $\log L_{1500\text{\AA}}^{\circ}(\text{erg s}^{-1} \text{\AA}^{-1})= 38.33$ , or  $\log L_{1500\text{\AA}}^{\circ}(\text{erg s}^{-1})= 41.51$  assuming  $\nu \times f_{\nu} \times 4\pi D^2$  as the monochromatic luminosity, belongs to the class of luminous super star clusters (SSCs) found at the heart of spirals (Carollo et al. 1997), and in nuclear

starburst galaxies (Meurer et al. 1995). At the derived age of 4 Myrs, the SSC in the nucleus of NGC 4303 is extremely luminous with a bolometric luminosity of about  $10^8 L_{\odot}$ , and an ionizing flux capable of producing an H $\alpha$  luminosity of up to about  $1.7 \times 10^{39}$  erg s $^{-1}$ , if all ionizing photons are absorbed by the surrounding interstellar medium.

The H $\alpha$  flux in the  $1''.0 \times 1''.0$  nuclear region along PA220 corresponds to a luminosity of  $1.2 \times 10^{39}$  erg s $^{-1}$ , after correcting for an stellar absorption of  $1.8\text{\AA}$  (equivalent width), and after slit/seeing aperture correction effects have been taken into account. The ratio of the predicted H $\alpha$  flux emitted by the SSC to the measured nuclear H $\alpha$  flux is 1.4. Therefore no additional ionizing source other than the SSC itself is required to explain the ionized gas luminosity.

#### 4.2. NGC 4303 nucleus: coexisting star clusters and AGN

As mentioned above, no evidence for a second energy source is present in the ultraviolet spectrum of the nucleus. However, its absolute optical magnitude  $M_{F606W} = -14.2$  and very red nuclear colors  $m_{F606W} - m_{F160W} = +3.5$  obtained from HST  $0''.2$  radius aperture measurements with filters WFPC2/F606W and NIC2/F160W<sup>3</sup> (see also Colina & Wada 2000), can not be explained by the emission due to the unobscured UV-bright SSC. According to the STARBURST99 models (Leitherer et al. 1999), the 4 Myrs,  $10^5 M_{\odot}$  UV-bright cluster should have an absolute visual magnitude of about  $-13$ , i.e. three times fainter than measured, and an optical – near-infrared color  $V-H \sim +0.2$ , i.e. much bluer than measured. Optical emission lines could affect the measured F606W magnitude, and

---

<sup>3</sup>Although filters F606W and F160W have a broadband profile different from the standard ground-based V and H filters, their effective wavelengths are very similar and consequently we adopt here the same names for simplicity.

therefore the observed V–H color could not represent the intrinsic continuum value, that would be even redder than observed. The WFPC2/F606W filter is an extreme broad-band filter with a bandpass of almost  $1600\text{\AA}$  that includes all the optical emission lines in the  $4800\text{\AA}$  to  $7000\text{\AA}$  spectral range. The predicted equivalent widths of the Balmer lines produced by a 4 Myr cluster are about  $100\text{\AA}$  and  $400\text{\AA}$  for  $H\beta$  and  $H\alpha$ , respectively (Leitherer et al. 1999). However, the ionized region centered on the nucleus is extended over about  $1''.5$ , as traced by the angular size of the  $\text{Ly}\alpha$  emission line region in our STIS long-slit spectrum. Moreover, the combined equivalent width of the nuclear  $[\text{NII}]+\text{H}\alpha$  line complex, as measured in our WHT spectrum of the nuclear region, corresponds to about  $20\text{\AA}$  indicating dilution by the bulge starlight contribution, that dominates the optical continuum in our ground-based spectrum. In summary, the contribution of the optical emission lines to the measured nuclear F606W flux is not expected to be more than a few percent.

The nuclear  $m_{F606W}-m_{F160W}$  color is also redder than the average bulge’s color in face-on spirals ( $V-H= 2.71 \pm 0.33$ ; de Jong, & van der Kruit 1994) and therefore, the presence of an additional red and luminous source has to be invoked. This additional source could either be an intermediate/old stellar population associated with the bulge, an evolved starburst dominated by red supergiants (about 10 Myr), or an accreting black hole. In the following these alternatives are discussed.

The first possibility would be that the bright near-infrared source traces the presence of an intermediate/old nuclear star cluster. Optical HST imaging has shown that many nearby spirals harbor nuclear star clusters, with a small fraction (about 5%) being unresolved (Carollo et al. 1997). Our long-slit optical continuum integrated over  $1''.0 \times 1''.0$  seems indeed to be dominated by an evolved stellar population around 1-5 Gyr old, with a total initial mass around  $10^8 M_{\odot}$  (Salpeter IMF normalized between 1 and  $100 M_{\odot}$ ). Even

allowing for some reddening ( $E(B-V)$  of 0.4 and 0.1 for both ages, respectively), the V–H color of this population wouldn't be redder than around 2.5, not being able to explain completely the observed infrared luminosity.

The excess H-band luminosity could also originate, at least partially, from a population of red supergiant stars formed in a previous starburst episode around 10 Myr ago (Cerviño & Mas-Hesse 1994; Leitherer et al. 1999), so that a two-stage starburst consisting of 4 + 10 Myr old stars within a few pc could coexist in the nucleus of NGC 4303. This scenario of a two-stage starburst is reminiscent of the star formation observed in the central 0.5 pc of the Milky Way and in NGC 1569, where a recent 4–8 Myr starburst, fully accounting for the ionizing and bolometric luminosities, coexist with an older cluster (Krabbe et al. 1995; Gonzalez Delgado et al. 1997). If a 10 Myr cluster were the dominating source of the luminous H-band point source ( $M_{F160W} = -17.7$ ) in NGC 4303, it would have had a mass of about  $2 \times 10^6 M_{\odot}$ . If we include the H-band luminosity associated with the very intermediate/old ( $> 1$  Gyr) stellar population, a starburst of about  $5 \times 10^5 M_{\odot}$  would be required. In either case, such a massive, unobscured cluster would produce an ultraviolet flux in excess of what is observed, and would produce a much bluer optical continuum than observed. Therefore, if the 10 Myr old starburst were present, it should be very significantly obscured both in the optical and ultraviolet ranges, with its associated light emerging only in the infrared, if at all.

Finally, the nuclear, luminous near-infrared source could alternatively indicate the presence of an AGN. The radiation emitted by the accreting black hole would dominate the energy output in the near and mid-infrared, as in most Seyfert 2 galaxies (Alonso-Herrero et al. 2001). Recent near-infrared imaging with HST has shown that all surveyed Seyfert 1 and 50% of the Seyfert 2 galaxies contain a luminous unresolved continuum source at  $1.6 \mu\text{m}$  (Quillen et al. 2001). The H-band luminosity of the NGC 4303 nucleus ( $M_{F160W} = -17.7$ )

agrees with the average value obtained by Quillen and collaborators for the subsample of Seyfert 2 galaxies with unresolved nuclear sources. There are additional independent indications that an accreting black hole exist in the nucleus of NGC 4303. The ground-based optical spectrum of the nuclear region ( $\sim 100$  pc) have line ratios anywhere between weak-[O I] LINERs and Seyfert 2 galaxies (see Table 1). However, the strongest evidence for an accreting black hole might come from recent *Chandra* images (Jiménez-Bailón et al. 2002, in preparation) that reveal the presence of an unresolved hard X-ray (2–10 keV) power-law source astrometrically coincident with the UV-bright nucleus, and similar in luminosity to other LLAGNs recently studied with *Chandra* (Ho et al. 2001). Following recent determinations of the black hole mass to velocity dispersion relationship (Ferrarese & Merritt 2000; Tremaine et al. 2002), the central velocity dispersion of  $74 \text{ km s}^{-1}$  (Heraudeau & Simien 1998) implies a mass of 1.2 to  $2.5 \times 10^6 M_{\odot}$  for the central black hole in NGC 4303. Given this mass, the X-ray accreting black hole would radiate very unefficiently, at extremely low sub-Eddington luminosities as in other LLAGNs (Terashima et al. 2000).

In summary, the high spatial resolution multifrequency studies done so far, give the first hints of the very complex structure of the central 10 pc of NGC 4303 where a young, luminous SSC apparently coexists with a low efficiency accreting black hole and with an intermediate/old star cluster. The young SSC is the dominant ionizing source, the accreting black hole is a minor contributor to the overall ionization and the old cluster contributes substantially to the optical and near-ir flux. Some additional red supergiant stars associated with an evolved starburst could also contribute to the near-infrared continuum.

#### 4.3. Implications for LLAGNs: the SSC–AGN connection

Low-luminosity AGNs as the one identified in the nucleus of NGC 4303, make up the vast majority of the AGN population (Ho, Filippenko & Sargent 1997). The empirical

evidence obtained so far indicates that a powerful SSC seems to coexist with an accreting black hole within the central 3 pc of NGC 4303. SSCs as the one detected in NGC 4303 are a common phenomenon in the nuclear regions of early and late-type spirals (Carollo et al. 1997; Carollo, Stiavelli & Mack 1998; Carollo et al. 2002; Boeker et al. 2002), and in galaxies with nuclear starbursts and circumnuclear star-forming rings (Meurer et al. 1995; Maoz et al. 1996). Therefore SSCs are a natural consequence of the star formation processes in the nuclear regions of spirals. On the other hand, the tightness of the black hole mass and stellar velocity dispersion relation (Ferrarese & Merritt 2000 and references; Tremaine et al. 2002) implies a link between massive black holes (MBH) and bulge formation in galaxies, and therefore nuclear MBHs should also be a natural consequence of the physical processes that formed present-day galaxies. So, it is reasonable to hypothesize that, as detected in the LLAGN NGC 4303, powerful SSCs could coexist with MBHs in the nucleus, i.e. inner few parsecs, of a large fraction of spirals. Under this hypothesis, at least some types of LLAGNs could be understood primarily as a consequence on one hand of the age and mass of the SSC, and on the other hand of the accretion rate and mass of the BH. Massive SSCs with masses of  $10^5$  to  $10^6 M_{\odot}$  would have peak bolometric luminosities of 0.2 to  $2 \times 10^9 L_{\odot}$  at an age of 3 Myrs. The associated, unobscured,  $H\alpha$  luminosities produced in the ionized interstellar medium surrounding the SSC would be in the 0.14 to  $1.4 \times 10^{40}$  erg  $s^{-1}$  range. On the other hand, low mass black holes such as the one in NGC 4303 (see §4.2) surrounded by accretion disks radiating at extremely low sub-Eddington luminosities ( $\sim 10^{-4} - 10^{-5} L_E$ ; Terashima et al. 2000), would emit bolometric luminosities of  $10^6$  to  $10^7 L_{\odot}$ , i.e. a factor of hundred less than a young SSC.

Therefore some types of LLAGNs could be understood as the result of the combined ionizing radiation emitted by an evolving super star cluster (i.e. determined by the mass and age) and an accreting black hole (i.e. radiating at sub-Eddington luminosities), coexisting in the inner few parsecs region. The SSC would have an ionizing spectral energy

distribution peaking in the soft X-rays/far-UV while the accreting black hole would have a harder radiation field with substantial flux beyond 1 keV. The nucleus of NGC 4303 with a central young (3-4 Myr old) SSC dominating its ionizing output in the inner few parsecs region, could be a prototype of the class of weak-[O I] LINERs. The LINER/HII nucleus in NGC 4569 could be another example of SSC-dominated LLAGN (Maoz et al. 1998; Barth & Shields 2000; Grabel & Bruhweiler 2002). On the other hand, LLAGNs like classical LINERs, or even low luminosity Seyfert 2 nuclei, could still host an evolved, i.e. 10 Myr or older, nuclear stellar cluster that will have a minor contribution to the ionizing luminosity, dominated therefore by an accreting black hole.

#### **4.4. Implications for LLAGNs: measuring the low-end of the black hole mass function**

The complementary multifrequency study of the nucleus of NGC 4303 has shown that stellar clusters of different ages seem to coexist with a black hole in the central few parsecs region of this LLAGN. Even the best  $0''.1$  spatial resolution available with HST STIS spectrograph represents a linear resolution of 10 pc at a distance of 20 Mpc, not enough to resolve the sphere of influence of nuclear black holes with masses of less than  $10^7 M_{\odot}$ . Therefore, the mass contribution of massive young SSCs as the one detected in NGC 4303, and of massive, compact, intermediate/old nuclear stellar clusters in spirals with central low mass black holes (masses of a few million solar masses as in the Milky Way, or as the estimated in NGC 4303, see section §4.2) could not be negligible and has to be taken into account. Black hole mass measurements are generally done under the assumption that the mass to light ratio of the stars is the same for all spirals, and spatially constant over the region used for the measurement (Sarzi et al. 2001; Sarzi et al. 2002). This might not be a bad assumption for ellipticals, but spirals could have large differences, in M/L, or even

gradients within same galaxy, if there are young nuclear clusters of different ages. NGC 4303 is a clear example of a spiral where the assumption of constant M/L would not be valid. Therefore, kinematical studies based on the analysis of optical emission lines alone can not provide the mass contribution of nuclear clusters, and therefore additional detailed multifrequency modeling and spectroscopy with HST would be required before deriving any reliable mass for central black holes with masses of a few to several million solar masses.

## 5. Summary

The main results presented in this paper can be summarized as follows:

(1) New HST ultraviolet STIS spectrum of the nucleus of the galaxy NGC 4303, classified as a LLAGN in the optical, shows unambiguously the presence of broad and intense P Cygni lines characteristic of young, massive stars and do not show any evidence of the strong UV emission lines characteristic of classical AGNs like NGC 1068.

(2) The ultraviolet properties of the nuclear cluster correspond to that of a compact (3.1 pc), young (4 Myrs), massive ( $10^5 M_{\odot}$ ), and luminous ( $\log L_{1500\text{\AA}}^{\circ}(\text{erg s}^{-1} \text{\AA}^{-1}) = 38.33$ ) star cluster. These properties are characteristic of the so called super star clusters (SSCs) commonly detected in the (circum-)nuclear regions of spirals and starburst galaxies.

(3) The SSC is the dominant ionizing source in the nucleus of NGC 4303. The ionizing energy produced by this cluster exceeds the flux needed to explain the extinction corrected nuclear H $\alpha$  luminosity, and therefore an additional non-thermal ionizing source is not required.

(4) New ground-based optical spectrum of the nuclear region (100 pc  $\times$  100 pc) favors the classification of the LLAGN as a weak-[O I] LINER although previous classification identified it as a LINER/Seyfert 2 borderline LLAGN. Scheduled HST observations will

establish the final classification.

(5) Circumnuclear stellar clusters at distances of 170 to 230 pc from the nucleus have similar ultraviolet spectra showing the broad and intense P Cygni lines characteristic of young, massive stars. These clusters are however a bit younger (3 to 3.5 Myr) and less massive ( $7-8 \times 10^3 M_{\odot}$ ) than the SSC detected in the nucleus.

(6) Additional multifrequency studies give the first hints of the very complex structure of the nucleus, i.e. region of a few pc in radius, of NGC 4303 where the SSC apparently coexist with a low efficiency accreting black hole and with an intermediate/old ( $> 1$  Gyr) compact star cluster, and where in addition an evolved ( $\sim 10$  Myr) starburst could also be present.

If the structure detected in the nucleus of NGC 4303 were common in spirals, there are two important implications that deserve further investigation:

(i) Some types of LLAGNs should be understood as the result of the combined ionizing radiation emitted by an evolving super star cluster (i.e. determined by the mass and age) and an accreting black hole (i.e. radiating at sub-Eddington luminosities), coexisting in the inner few parsecs region. Under this scheme, the ionization in LLAGNs classified as LINER/HII nuclei or weak-[O I] LINERs would be dominated by a young (3-4 Myrs) super star cluster. Classical LINERs and low-luminosity Seyfert 2 could still host an older ( $\geq 10$  Myrs) cluster but the ionizing continuum would be dominated by an accreting black hole.

(2i) For spirals containing low mass (i.e. less than few to several  $10^6 M_{\odot}$ ) nuclear black holes, the contribution of massive nuclear clusters to the dynamical mass within the inner 10 pc region has to be established accurately before deriving any firm conclusion about the mass of the black hole.

LC, RGD, and JMMH acknowledges support by the Spanish Ministry of Science

and Technology (MCYT) through grants PB98-0340-C02, AYA-2001-3939-C03-01 and AYA-2001-3939-C03-02. The authors want to thank the anonymous referee for his/her excellent report that has largely improved the clarity and content of the paper. This research was supported by grant GO-08665.01-A from the Space Telescope Science Institute. Authors thank the staff at El Roque de los Muchachos Observatory that obtained the optical spectra during the course of service observations with the William Herschel Telescope.

Table 1. Ultraviolet and optical properties of the nucleus and circumnuclear clusters

Region	$F_{UV}(1500\text{\AA})^a$	$E(B-V)^b$	$\log L_{UV}(1500\text{\AA})^c$	$\log([\text{O III}]/\text{H}\beta)^d$	$\log([\text{O I}]/\text{H}\alpha)^d$	$\log([\text{N II}]/\text{H}\alpha)^d$	$\log([\text{S II}]/\text{H}\alpha)^d$
Nucleus	3.40	0.07 (0.10)	38.33	0.28	-1.35	0.06	-0.32
		0.0		0.50	-0.96	0.01	-0.31
Cluster G	0.84	0.10 (0.15)	37.85	-0.37	-	-0.27	-0.54
		0.1		-0.72	-	-0.35	-0.64
Cluster L	0.25	0.10 (0.15)	37.33	-	-	-	-

<sup>a</sup>Observed ultraviolet flux, not corrected for extinction, in units of  $10^{-15} \text{ erg s}^{-1} \text{ cm}^{-2} \text{ \AA}^{-1}$ .

<sup>b</sup>Internal extinction. First row gives the value as derived from the UV spectra considering an LMC extinction curve. Values in parenthesis were derived using Calzetti’s law (Calzetti et al. 2000). Second row presents the value derived from the  $\text{H}\alpha/\text{H}\beta$  ratios.

<sup>c</sup>Extinction-corrected luminosity using the listed  $E(B-V)$  values in units of  $\text{erg s}^{-1} \text{ \AA}^{-1}$ .

<sup>d</sup>Extinction-corrected emission line ratios. In addition to the hydrogen Balmer lines, the collisionally-excited lines used are  $[\text{O III}]$  5007Å,  $[\text{O I}]$  6300Å,  $[\text{N II}]$  6584Å, and the  $[\text{S II}]$  doublet 6717,6731Å. First row of values as derived from the long-slit WHT/ISIS spectrum using an aperture of  $1'' \times 1''$ . Second row are the values derived from previous integral field spectroscopy (Colina & Arribas 1999). The spectrum for cluster L, at a distance of  $0.''6$  from cluster G, can not be obtained in ground-based spectroscopic observations.

Table 2. Modeled properties of the nuclear and circumnuclear stellar clusters

Region	IMF index	Age (Myrs)	Mass ( $10^4 M_{\odot}$ )	$\log Q_{model}^a$ (ph s $^{-1}$ )	$\log Q_{H\alpha}^b$ (ph s $^{-1}$ )
Nucleus	2.35	4.0	10.0	51.10	50.9
Cluster G	1.50	3.0	0.7	51.04	50.4
Cluster L	2.35	3.5	0.8	50.22	–

<sup>a</sup> $Q_{model}$  is derived integrating the synthetic spectral energy distribution of the modeled clusters for photons with energies above 13.6 eV

<sup>b</sup>Derived from the WHT/ISIS H $\alpha$  flux after correction for stellar absorption and aperture effects, and assuming  $Q_{H\alpha}$  is given as  $7.5 \times 10^{11} \times L(H\alpha)$  ph s $^{-1}$

## REFERENCES

- Allen, M.G., Dopita, M.A., & Tsvetanov, Z.I. 1998, ApJ 493, 571
- Alonso-Herrero, A., Quillen, A.C., Simpson, C., Efstathiou, A., & Ward, M.J. 2001, AJ 121, 1369
- Barth, A.J., Ho, L.C., Filippenko, A.V., & Sargent, W.L.W. 1998, ApJ 496, 133
- Barth, A.J., & Shields, J.C. 2000, PASP 112, 753
- Boeker, T., Laine, S., van der Marel, R.P., Sarzi, M., Rix, H.W., Ho, L.C., Shields, J.C. 2002, AJ in press (astro-ph/0112086)
- Calzetti, D., Armus, L., Bohlin, R.C., Kinney, A.L., Koornneef, J., & Storchi-Bergmann, T. 2000, ApJ 533, 682
- Carollo, C.M., Stiavelli, M., de Zeeuw, P.T., & Mack, J. 1997, AJ 114, 2366
- Carollo, C.M., Stiavelli, M., & Mack, J. 1997, AJ 116, 68
- Carollo, C.M., Stiavelli, M., Seigar, M., de Zeeuw, P.T., & Dejonghe, H. 2002, AJ 123, 159
- Cerviño, M., & Mas-Hesse, J.M. 1994, AA 284, 749
- Cid Fernandes, R., Heckman, T., Schmitt, H., González Delgado, R., & Storchi-Bergmann, T. 2001, ApJ 558, 81
- Colina, L., & Arribas, S. 1999, ApJ 514, 637
- Colina, L., García-Vargas, M., González-Delgado, R., Mas-Hesse, J.M., Pérez, E., Alberdi, A., & Krabbe, A. 1997a, ApJ 484, L41
- Colina, L., García-Vargas, M., Mas-Hesse, J.M., Alberdi, A., & Krabbe, A. 1997b, ApJ 484, L41

- Colina, L., & Wada, K. 2000, ApJ 529, 845
- Crenshaw, D.M. & Kraemer, S. B. 2000, ApJ 532, 247
- de Vaucouleurs, G., de Vaucouleurs, A., Corwin, H.G., Buta, R.J., paturel, G., & Fouque, P. 1991, Third Reference Catalogue of Bright Galaxies (Berlin: Springer)
- Eracleous, M., Shields, J.C., Chartes, G., & Moran, E.C. 2002, ApJ 565, 108
- Ferrarese, L., & Merritt, D. 2000, ApJ 539, L9
- González Delgado, R., Leitherer, C., Heckman, T., & cerviño, M. 1997, ApJ 483, 705
- González Delgado, R., Heckman, T.M. et al. 1998, ApJ 505, 174
- Grabel, J.R., & Bruhweiler, F.C. 2002, AJ in press (also astro-ph/0204371)
- Heckman, Y.M., González Delgado, R. et al. 1997, ApJ 482, 114
- Heraudeau, Ph., & Simien, S. 1998, AASS 133, 317
- Ho, L.C., Filippenko, A.V., & Sargent, W.L.W. 1997, ApJ 487, 568
- Ho, L.C., et al. 2001, ApJ 549, L51
- Krabbe et al. 1995, ApJ 447, L95
- Krist, J., & Hook, R. 2001, The Tiny Tim User's Guide. Version 6.0. STScI.
- Leitherer, C., Schaeder, D., Goldader, J.D., González-Delgado, R., Robert, C., Foo Kune, D., de Mello, D.F., Devost, D., & Heckman, T. 1999, ApJS 123, 3
- Maoz, D., Barth, A.J., Sternberg, A., Filippenko, A.V., Ho, L.C., Macchetto, F.D., Rix, H.-W., & Schneider, D.P. 1996, AJ 111, 2248

Maoz, D., Koratkar, A., Shields, J.C., Ho, L.C., Filippenko, A.V., & Sternberg, A. 1998, AJ 116, 55

Mas-Hesse, J.M., & Kunth, D. 1999, A&A 349, 765

Meurer, G.R., Heckman, T.M., Leitherer, C., Kinney, A., Robert, C., & Garnett, D.R. 1995, AJ 110, 2665

Norman, C., & Scoville, N. 1988, ApJ 332, 124

Quillen, A.C., McDonald, C., Alonso-Herrero, A., Lee, A., Shaked, S., Rieke, M.J., & Rieke, G.H. 2001, ApJ 547, 129

Sarzi, M. et al. 2001, ApJ 550, 65

Sarzi, M. et al. 2002, ApJ 567, 237

Schinnerer, E., Mcejewski, W., Scoville, N., & Moustakas, L.A., 2002, ApJ in press (also astro-ph/0204133)

Shapiro, S.L., & Teukolsky, S.A. 1985, ApJ 292, L41

Terashima, Y., Ho, L.C., Ptak, A.F., Mushotzky, R.F., Serlemitsos, P.J., Yaqoob, T., & Kunieda, H. 2000, ApJ 533, 729

Tremaine, S., et al. 2002, ApJ in press (also astro-ph/0203468)

Vacca et al. 1995, ApJ 444, 647

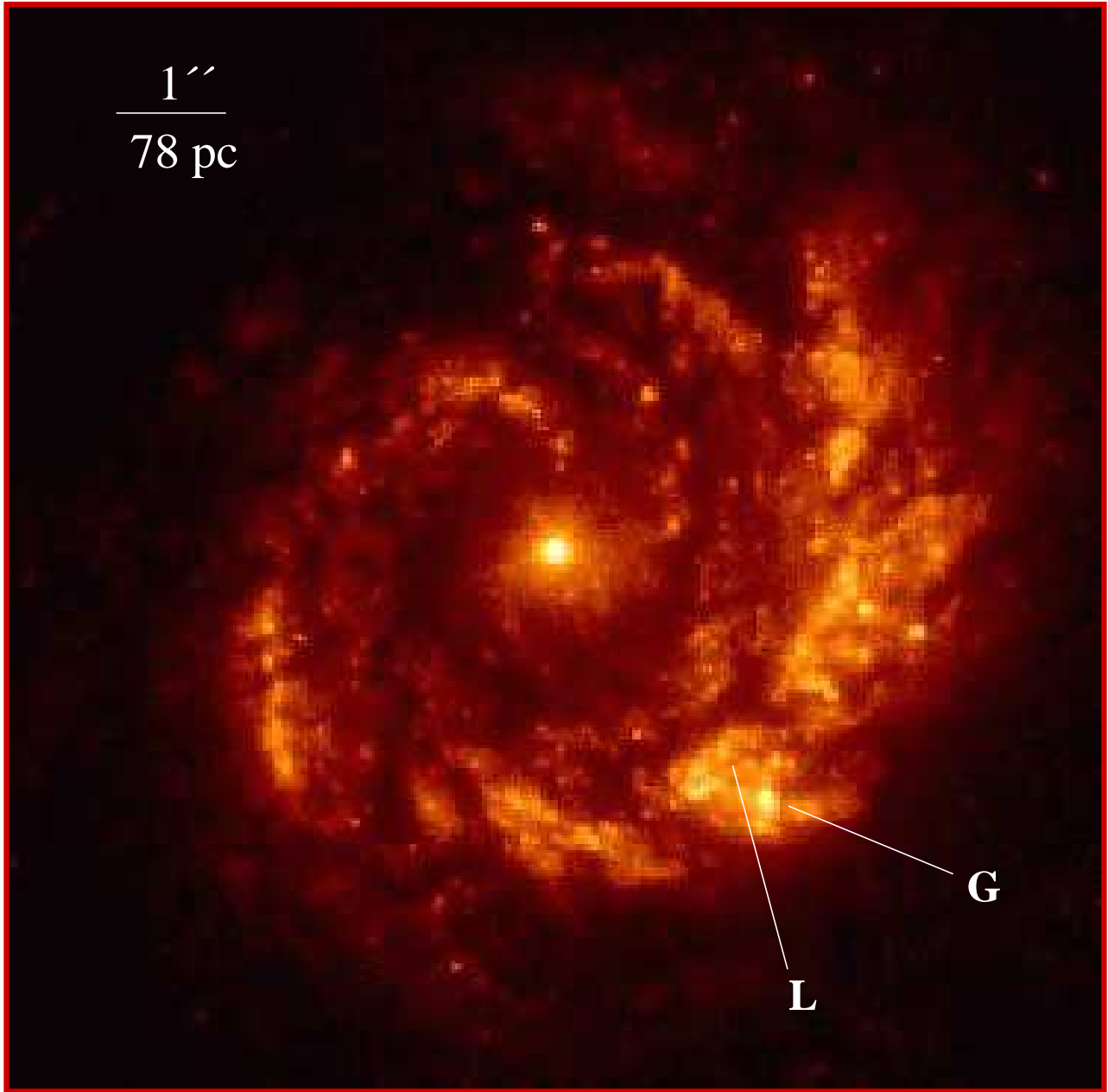


Fig. 1.— STIS F25QTZ ultraviolet image of NGC 4303 nucleus and the surrounding star-forming spiral structure, already detected in a previous WFPC2 image (Colina et al. 1997b). The positions of clusters G and L detected in our long slit STIS spectrum are indicated for reference. North is up and east to the left.

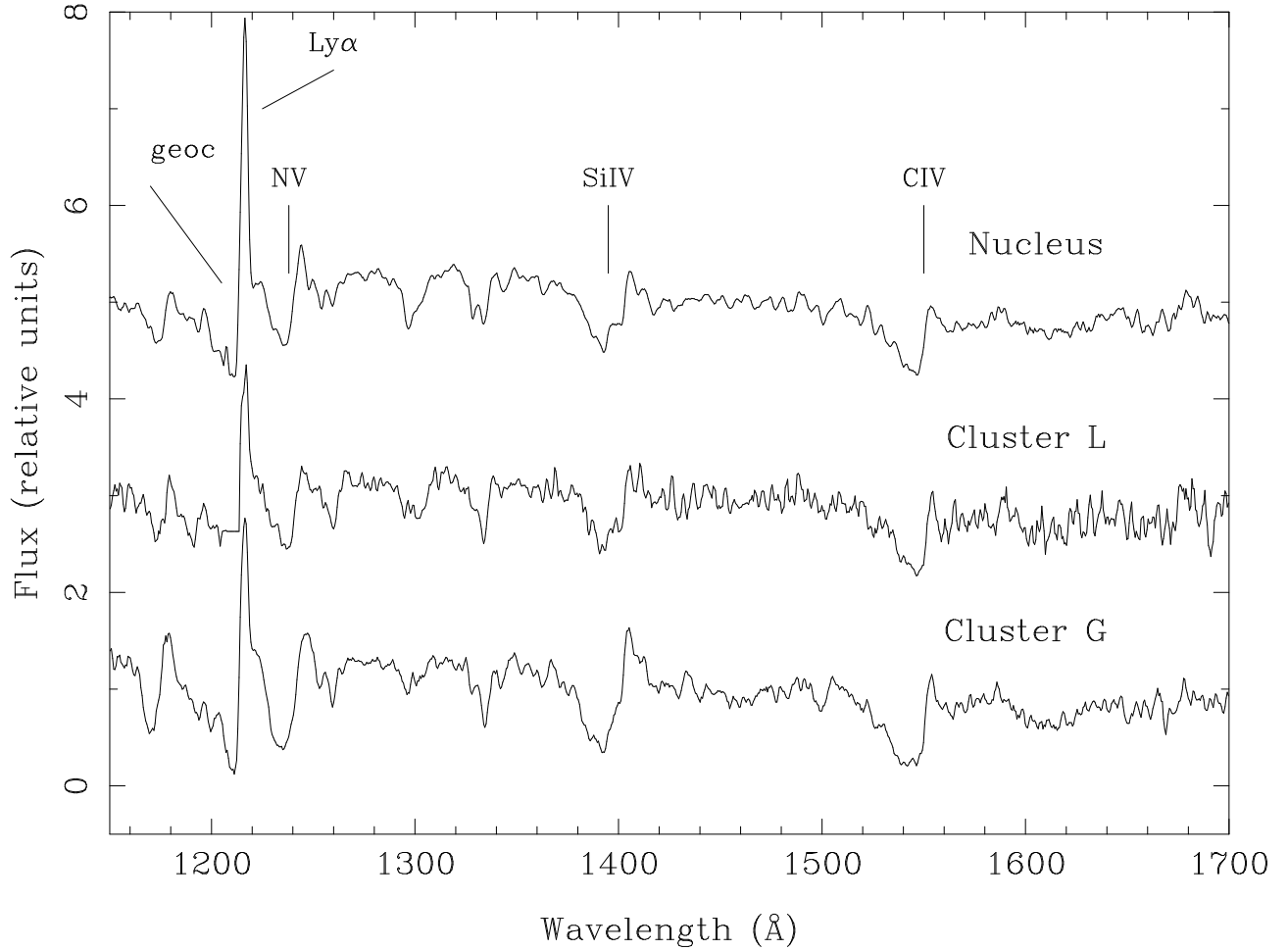


Fig. 2.— Rest-frame STIS UV spectra of the nucleus and circumnuclear clusters G and L. The three spectra show the characteristic broad P Cygni lines (N V 1240Å, Si IV 1400Å, C IV 1550Å) produced by the winds of massive young stars. In addition, the three spectra show a narrow Ly $\alpha$  line in emission but no trace of other emission lines like Si IV 1400Å and C IV 1550Å, typical of luminous Seyferts.

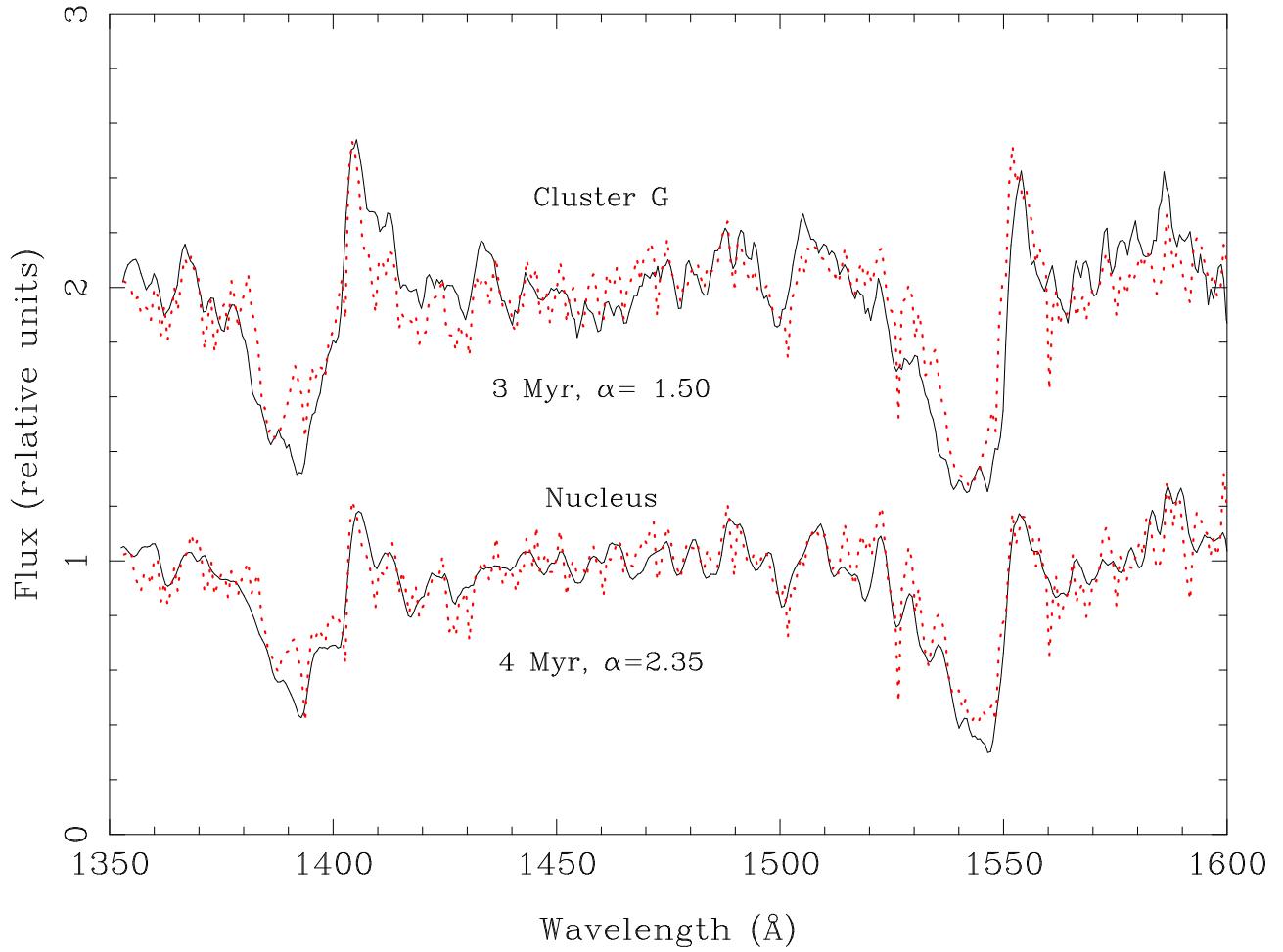


Fig. 3.— Rest-frame STIS UV spectra of the nucleus and cluster G, centered on the Si IV 1400Å and C IV 1550Å lines, are shown (thin continuous line). The best fitted instantaneous starburst model for the observed spectra are superimposed (dotted lines). The age and slope of the IMF for each of the modeled clusters are also indicated.

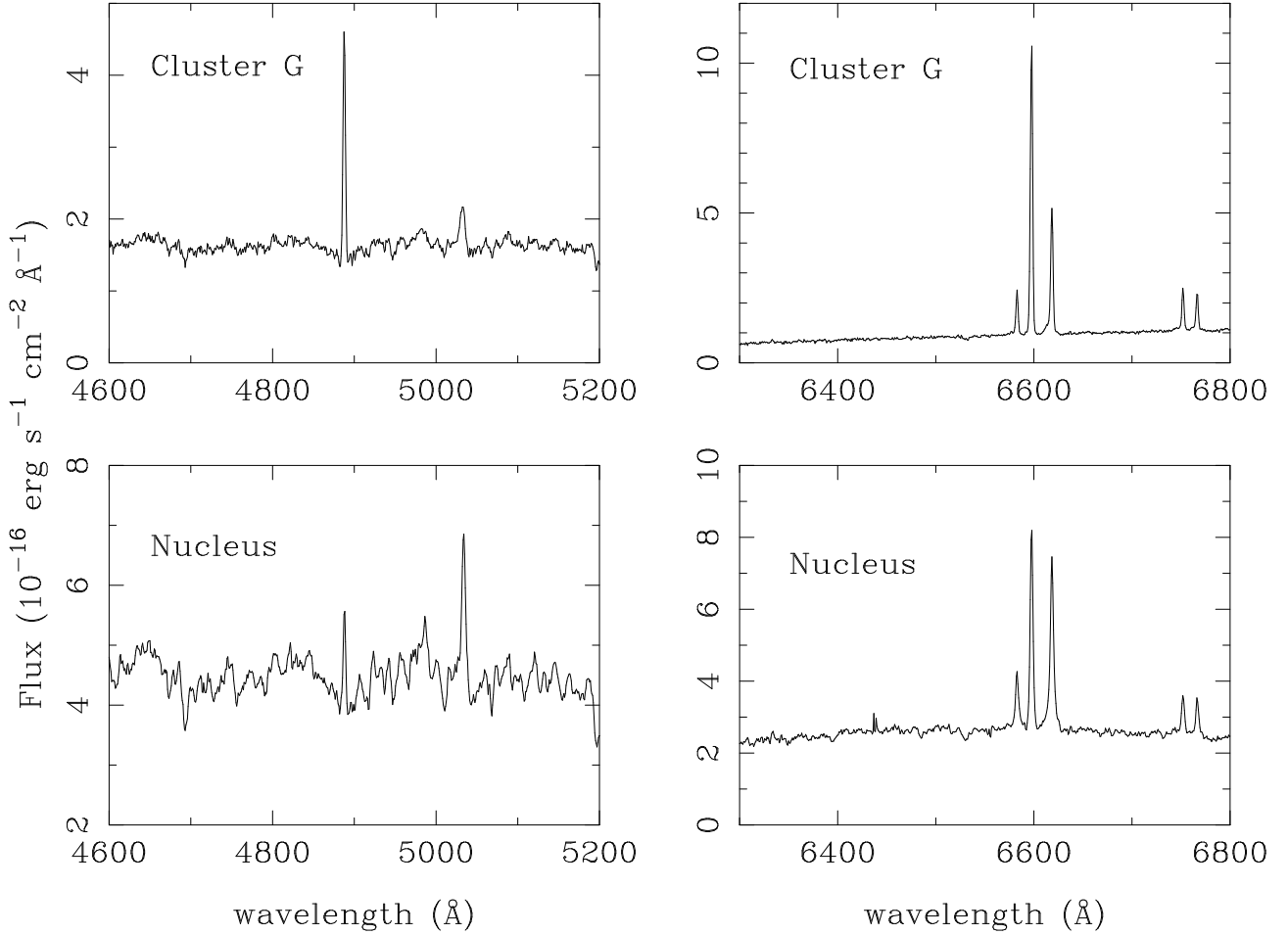


Fig. 4.— WHT optical observed spectra of the nucleus and cluster G illustrating the different excitation conditions in these regions as traced by the changes in the observed ratios of the optical emission lines. The left-side plots show the H $\beta$  and [O] III 4959,5007 $\text{\AA}$  part of the spectra while the right-side plots present the H $\alpha$ , [N] II 6548,6584 $\text{\AA}$  and the [S] II 6717,6731 $\text{\AA}$  lines. The wavelength axis indicates the observed wavelength, not redshift corrected.